

# Mode-locked Yb:KGW laser longitudinally pumped by polarization-coupled diode bars

Gary R. Holtom

*Environmental Molecular Sciences Laboratory, Pacific Northwest National Laboratory, Richland, Washington 99354*

Received June 7, 2006; accepted June 28, 2006;  
 posted July 7, 2006 (Doc. ID 71742); published August 25, 2006

Mode-locked operation of a simple Yb:KGW (potassium gadolinium tungstate) oscillator is described, providing 10 W at 1039 nm with a 290 fs pulse width. A polarization-coupled scheme is used for efficient longitudinal pumping by a pair of reshaped laser diode bars. With changes in cavity dispersion, the pulse width is adjustable from 134 to 433 fs, in a high-quality circular mode. A saturable absorber mirror provides self-starting operation, and the cavity is stabilized by the Kerr-lens effect. © 2006 Optical Society of America  
 OCIS codes: 140.3480, 140.3580, 140.4050, 140.5680.

The large spectral linewidth of Yb in crystalline hosts, as compared with Nd, permits solid-state laser operation with subpicosecond pulses, using direct diode pumping.<sup>1</sup> Since Yb is a quasi-three-level system, higher-intensity pumping is required than for Nd lasers, but the thermal effects in Yb lasers are reduced as a consequence of a smaller quantum defect.<sup>2</sup> A variety of crystalline hosts have been described, with the tungstate hosts having large optical cross sections, a desirable property for diode pumping.<sup>3</sup> The highest reported average power for mode-locked (ML) operation using a single element gain medium with a simple pump geometry is about 1 W. In one scheme, the Brewster angle crystal is pumped from both sides by a pair of single emitter diodes delivering a few watts of pump light at the 981 nm absorption maximum.<sup>1</sup> In another scheme, a flat plate is pumped from one side at near-normal incidence.<sup>4</sup> While much higher powers in both continuous and ML operation have been reported for thin-disk<sup>5</sup> and fiber<sup>6</sup> technology, these systems are more complex than the simple, directly diode pumped sources. Here we show that directly pumped solid-state technology produces powers exceeding the ML Ti:sapphire laser.<sup>7</sup>

Laser diode bars are an efficient high-power pump source, and the challenge is to effectively couple the large number of emitters, usually 19 or more on a single 1 cm bar, into a single focusable spot. With more than 10 W of pump power, thermal management becomes important, even with the high quantum yield for fluorescence<sup>2</sup> of Yb:KGW (potassium gadolinium tungstate) and the low quantum defect of 6% between the 981 nm pump and the 1040 nm lasing wavelength. On-axis longitudinal pumping also allows a thin slab with low doping of Yb, to maximize heat removal and minimize the temperature rise in the pumped region.

Many of the reported Yb:KGW and the similar Yb:KYW (potassium ytterbium tungstate) lasers employ large optical absorption and emission cross sections that are polarized parallel to the crystal *a* axis. The *b* axis has a much smaller absorption cross section than the *a* axis, but at 1040 nm the *b* axis emission cross section is comparable with the *a* axis and

has a broader bandwidth.<sup>8</sup> Absorption losses at the lasing frequency along the *b* axis are also smaller than along the *a* axis. Optical anisotropy inherent in the low-symmetry monoclinic tungstate crystal allows an efficient scheme using polarizers to couple the relatively divergent pump laser into the cavity, overcoming limiting geometric factors in making a practical laser. This design uses a dielectric mirror to reflect *s*-polarized light at 981 nm and to transmit the *p*-polarized laser radiation near 1040 nm, providing an efficient means for introducing pump light into the cavity.<sup>9</sup> The crystal is a 10 mm square slab, with near-normal-incidence longitudinal pumping through the antireflection-coated sides. The *a* axis is vertical, and the *b* axis is horizontal. The slab is 1.4 mm thick and is mounted vertically between water-cooled plates, using indium foil for efficient heat transfer. The crystal was obtained from NovaPhase and has a doping of 1.5%. The long absorption path in the crystal and low doping reduce the temperature rise at the edges of the crystal but also require care to match the divergence of the diode pump beam over the long beam overlap region.<sup>10</sup>

The collimation optics in the laser diode package (Apollo Instruments Model S14-981-1) increase the effective optical brightness of the laser diode bar by reshaping the beam, stacking the 0.5-mm-wide magnified images of individual emitters into an  $\sim 7$  mm  $\times$  11 mm rectangular near-field beam, at a nominal beam divergence of 3 mrad in each direction. Each pump laser provides 23 W at the drive current of 35 A used for this work. The output beam of the water-cooled diode package is small enough to directly couple to the gain medium. The beam is highly polarized and is aligned vertically with a half-wave plate. Measured small signal diode light absorption in the crystal is 93% and is more than 98% at the absorption center wavelength.

While it is not necessary to use Brewster's angle in the design of the dielectric polarizer, it is convenient, since an antireflection layer on the rear surface is not required. Our mirrors have greater than 89% reflectivity at 981 nm and 99.3% transmission at 1038 nm. The cavity layout is shown in Fig. 1 and has four mirrors plus a saturable absorber mirror (SAM) provided

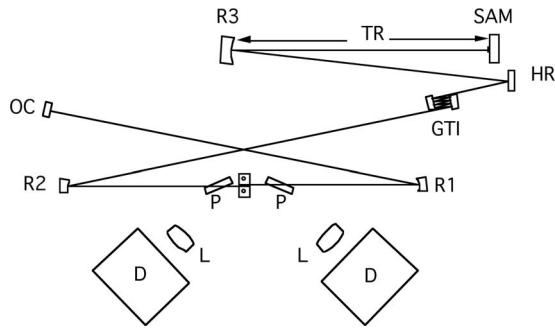


Fig. 1. Layout of laser. Reshaped diode bar assemblies D are focused by lenses L, and P are dielectric polarizers. The Yb:KGW crystal is mounted between water-cooled plates. The output coupler OC is flat, and the high reflectors R1 and R2 have 500 mm radii. The fold mirror R3 has a radius of 800 mm, and distance TR is adjusted for best power and stability. Negative dispersion is provided by the flat mirror pair GTI and mirrors R1 and R2. HR is a flat folding mirror. Distances are roughly to scale, but the size of parts is exaggerated.

by BATOP Optoelectronics (SAM-1040-1.5-25.4 s), and a flat folding mirror. The multiple bounce Gires-Tournois interferometer (GTI) mirror pair is supplied by Layertec GmbH to provide adjustable negative dispersion. This cavity has the flexibility required to independently control the spot sizes in the gain medium and the SAM, which is essential for the stable ML operation. The fold angles are as small as conveniently possible, typically  $3^\circ$ , making the cavity astigmatism negligible. Pump light is focused with 75 mm focal length achromatic lenses.

Obtaining a high-quality, diffraction-limited beam requires careful positioning of the laser diodes and lenses, and a good mode quality is achievable with a lasing radius between 100 and  $180 \mu\text{m}$  at the Yb:KGW crystal. The long arm is well collimated and is suitable for insertion of a GTI mirror pair. An output coupler with 78% reflectivity is used for pulses shorter than 250 fs, and an 84% coupler for the longer pulses. While this cavity has greater losses than other Yb diode-pumped lasers reported to date, the gain and power levels are also greater. Operation with a high-transmission output coupler reduces the effect of cavity losses, particularly from absorption losses leading to heating within the SAM.

An area of great concern with diode-pumped solid-state lasers is the extent of the thermal lens and the consequences of this lensing on cavity alignment and stability. The thermal lens in a strongly pumped Yb:KGW crystal has been reported to be as large as 10 diopters with 7 W of absorbed pump light.<sup>2</sup> However, the thermal lensing depends on thermo-optical properties that are highly anisotropic, and in certain directions the lensing is much reduced.<sup>11</sup> The thermal lensing under our lasing conditions was determined by systematically exploring the stability limits while lasing, using a symmetric four-mirror cavity. All spot sizes are calculated by using the inferred 4 diopter lens.

Producing stable mode locking is straightforward. The diode focus and overlap are optimized with cw lasing by using a beam radius in the Yb:KGW crystal

of about  $150 \mu\text{m}$  and a 78% reflecting output coupler. The cavity includes a translation stage for the most critical adjustment, the distance TR between the SAM and the fold mirror (Fig. 1). Initially the laser cavity is stable in cw operation with TR at 596 mm, as indicated by the solid curve in Fig. 2. Additional positive lensing from the nonlinear Kerr effect moves the cavity to point mode locking, where the laser self-starts with stable mode locking. The highest powers are reached by decreasing TR to 584 mm to reach point HP, which suppresses cw lasing. If the beam is interrupted, the laser will not self-start from HP, but restarts easily by momentarily pushing the translation stage to a longer distance. Pulse properties are substantially identical for three SAMs with a saturable absorbance of 0.7%, 1.0%, and 1.5%, indicating that soliton mode effects control the stabilized pulse train.

The two fold mirrors have a dispersion of  $-1300 \text{ fs}^2$ , enough to offset the positive material dispersion of the Yb:KGW. Additional dispersion is provided by a multiple bounce GTI flat mirror pair, with each reflection providing  $-1300 \text{ fs}^2$ . More than eight reflections can fit on each 25 mm GTI mirror. The spectral pulse width and measured pulse width vary linearly with total negative dispersion, as expected from soliton-mode theory.<sup>12</sup> The results are summarized in Table 1. In all cases, the spectra (Fig. 3A) and autocorrelation shapes (Fig. 3B) are smooth, and the pulses have a stable amplitude as observed with a fast diode and oscilloscope, until the mode locking is terminated by air currents or a mechanical vibration, typically on a time scale of many minutes.

The role of the nonlinear refractive index [Kerr lens mode locking (KLM)] in the stabilization of the ML pulse formation has been discussed frequently.<sup>13</sup> When the SAM is replaced by a high reflector, intense modulation is seen during mirror translation or mirror tapping, and in some cases bursts of ML pulses are observed. The process governing high-energy pulse development in this laser involves both the SAM and the KLM. The spectral and autocorrelation profiles of this laser, at all pulse widths, are similar to the reported "pure" KLM lasers.<sup>8,13</sup> The KGW crystal has a high refractive index,  $\sim 2.0$  for radiation polarized along the  $b$  axis, and a large nonlinear index has been reported.<sup>14</sup>

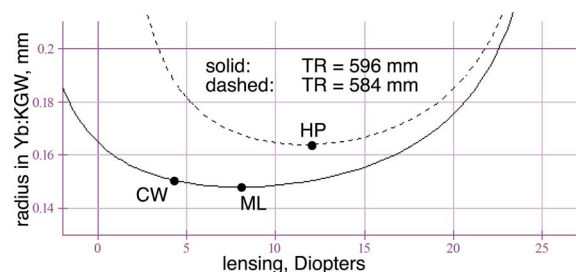


Fig. 2. Spot sizes in the Yb:KGW crystal and the SAM, as a function of total lensing. Cw lasing occurs at a thermal lensing of four diopters, point CW, and mode-locked operation moves to point ML. Higher powers are available at point HP, at shorter TR.

**Table 1. Performance Summary of the Laser**

GTI Reflections	GVD <sup>a</sup> (fs <sup>2</sup> )	SW <sup>b</sup> (nm)	T <sup>c</sup> (fs)	P <sup>d</sup> (W)
1	-6200	11.3	134	5.3
2	-14,600	6.0	228	8.6
4	-25,000	5.0	292	9.9
8	-45,800	3.1	433	10.0

<sup>a</sup>GVD is the estimated net round trip cavity dispersion.

<sup>b</sup>SW is the spectral half-width in nanometers.

<sup>c</sup>T is the measured pulse width, assuming a sech<sup>2</sup> deconvolution factor.

<sup>d</sup>P is the output power.

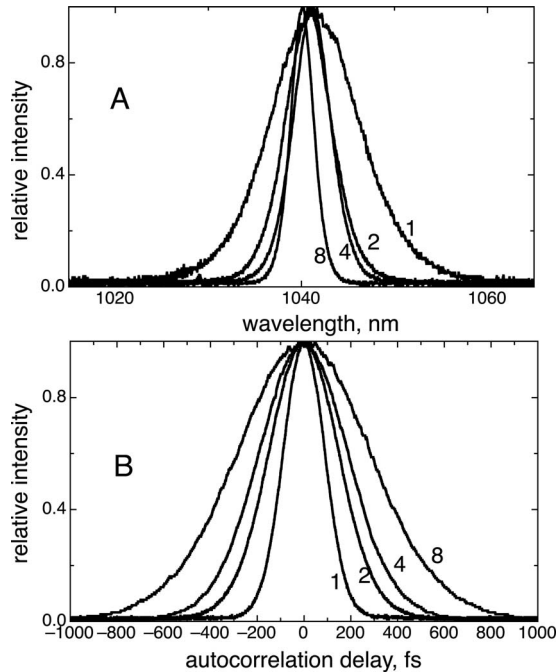


Fig. 3. A, Spectra and B, autocorrelation traces, plotted for the GTI reflections listed in Table 1.

No damage to the SAM is seen as long as the spot is larger than  $130\ \mu\text{m}$ , with the high transmission output coupler. Higher-reflectivity output couplers, and larger mode diameters in the Yb:KGW crystal, may result in optical damage, particularly during a Q-switching event. At our repetition rate of 45 MHz and power of 10 W, the pulse energy is greater than 200 nJ. Present powers are greater than Ti:sapphire ultrafast lasers, and the Yb:KGW laser does not require a high-quality visible pump laser. In addition, the pulse width can be easily adjusted over a wide range. Higher powers and shorter pulses have been observed with less robust polarizers, showing that

the reported performance can be improved. By scaling the spot sizes and mirror reflectivity, the laser is expected to provide output powers of several watts by use of inexpensive single emitter diode pump lasers, making a laser source well suited for multiphoton microscopy and nonlinear spectroscopy. Second-harmonic conversion efficiency exceeds 60% with a noncritically phase-matched LiB<sub>3</sub>O<sub>5</sub> crystal.

This work was supported by the U.S. Department of Energy Office of Basic Energy Sciences Division of Chemical Sciences, and the Office of FreedomCAR and Vehicle Technologies. The work was performed at the W. R. Wiley Environmental Molecular Science Laboratory, a national scientific user facility sponsored by the Office of Biological and Environmental Research, located at the Pacific Northwest National Laboratory. G. Holtom's e-mail address is gary.holtom@pnl.gov.

## References

1. F. Brunner, G. J. Spühler, J. Aus der Au, L. Krainer, F. Morier-Genoud, R. Paschotta, N. Liechtenstein, S. Weiss, C. Harder, A. A. Legatsky, A. Abdolvaud, N. V. Kuleshov, and U. Keller, *Opt. Lett.* **25**, 1119 (2000).
2. S. Chénais, F. Balembois, F. Druon, G. Lucas-Leclin, and P. Georges, *IEEE J. Quantum Electron.* **40**, 1235 (2004).
3. G. Boulon, *Opt. Mat.* **22**, 85 (2003).
4. A. Major, V. Barzda, P. A. E. Piunno, S. Musikhin, and U. J. Krull, *Opt. Express* **14**, 5285 (2006).
5. E. Innerhofer, T. Südmeyer, F. Brunner, R. Häring, A. Aschwanden, R. Paschotta, C. Hönninger, M. Kumkar, and U. Keller, *Opt. Lett.* **28**, 367 (2003).
6. F. Röser, J. Rothhard, B. Ortac, A. Liem, O. Schmidt, T. Schreiber, J. Limpert, and A. Tünnermann, *Opt. Lett.* **30**, 2754 (2005).
7. L. Xu, G. Tempea, Ch. Spielmann, F. Krausz, A. Stingl, K. Ferencz, and S. Takano, *Opt. Lett.* **23**, 789 (1998).
8. H. Liu, J. Nees, and G. Mourou, *Opt. Lett.* **26**, 1723 (2001).
9. K. R. German, *Opt. Lett.* **4**, 68 (1979).
10. Y. F. Chen, T. S. Liao, C. F. Kao, T. M. Huang, K. H. Lin, and S. C. Wang, *IEEE J. Quantum Electron.* **32**, 2010 (1996).
11. S. Biswal, S. P. O'Connor, and S. R. Bowman, *Appl. Opt.* **44**, 3093 (2005).
12. T. Brabec, Ch. Spielmann, and F. Krausz, *Opt. Lett.* **16**, 1961 (1991).
13. A. A. Lagatsky, A. R. Sarmani, C. T. A. Brown, W. Sibbett, V. E. Kisel, A. G. Selivanov, I. A. Denisov, A. E. Troshin, K. V. Yumashev, N. V. Kuleshov, V. N. Matrosov, T. A. Matrosova, and M. I. Kupchenko, *Opt. Lett.* **30**, 3234 (2005).
14. A. Major, I. Nikolakakos, J. S. Aitchison, A. I. Ferguson, N. Langford, and P. W. E. Smith, *Appl. Phys. B* **77**, 433 (2003).